INSTITUTE OF PHYSICS PUBLISHING JOURNAL OF PHYSICS: CONDENSED MATTER

J. Phys.: Condens. Matter **18** (2006) 5425–5434 doi:10.1088/0953-8984/18/23/014

Characterization of periodically nanostructured copper filaments self-organized by electrodeposition

Zhe Wu[1], Yong-Jun Bao[1], Guang-Wei Yu[2], Mu Wang[1,4], Ru-Wen Peng[1], Vincent Fleury[3], Xi-Ping Hao[1] and Nai-ben Ming[1]

[1] National Laboratory of Solid State Microstructures, Nanjing University, Nanjing 210093, People's Republic of China
[2] Institute of Crystalline Materials, Shangdong University, Jinan 250100, People's Republic of China
[3] Laboratoire de Physique de la Matière Condensée, Ecole Polytechnique, Palaiseau 91128, France

E-mail: muwang@nju.edu.cn

Received 11 February 2006, in final form 12 April 2006
Published 26 May 2006
Online at stacks.iop.org/JPhysCM/18/5425

Abstract

We report in this paper the electric properties of nanostructured copper filament arrays self-organized by a novel electrochemical method. Due to the spontaneous oscillation of the concentration field of $[Cu^{2+}]$ in front of the growing interface, crystallites of copper and cuprous oxide appear alternately on the filaments of the electrodeposits. A conducting atomic force microscope (CAFM) and current imaging tunnelling spectroscopy (CITS) were used to characterize the electric properties of the nanostructured copper filaments. By applying a constant voltage across the conducting probe of the CAFM and the sample, an electric current mapping is achieved, in which alternating low and high current regions correspond exactly to the periodic nanostructures on the filaments. The profile of the electric current along the structured filament has been analysed, and no noticeable potential drop has been observed. A typical linear I–V curve for a metal and nonlinear I–V curve for a semiconductor were collected in the high and low current regions respectively. These results suggest that despite the periodic distribution of Cu_2O crystallites on the deposited filament, there should exist a metallic core of copper crystallites inside the filament. This type of structured metal–semiconductor filament might have potential application.

1. Introduction

During the past decade the microelectronics industry has begun to switch rapidly from aluminium-based wiring to multilevel metal interconnects based on copper. This transition

[4] Author to whom any correspondence should be addressed.

is due to the fact that chips wired with copper have significant advantages in performance and manufacturing cost over those made with aluminium [1, 2]. In the microelectronics industry, the metallic interconnection is usually achieved via a 'top-down' photolithography process. To find new ways to form electric contacts in three dimensions and to achieve enhanced data-processing density, people have been trying to establish conducting channels between electrodes with patterned and direction-controlled electrodeposition [3, 4] and electropolymerization [5, 6]. Yet in previous reports the metal electrodeposit was usually ramified. A ramified metallic connection is clearly not favoured for microelectronics. The reason is that the random ramification of the deposited filaments may increase the electric capacitance of the system, which may countervail the benefit of lower electric resistance of copper wiring and slow down the switching speed of an RC circuit. An essential step towards the real application of patterned electrodeposition is to suppress the ramification of the deposits, and to gain efficient control over the deposit morphology [7–11].

To suppress the ramification of the deposit and to control the deposit morphology, we recently developed a unique electrodeposition method [12], which allows the copper electrodeposits to grow robustly on a glass substrate with considerably low branching rate. When the voltage across the electrode is kept constant (potentiostatic mode), copper filament arrays covered with periodic nanostructures of Cu and Cu_2O are obtained. Due to the fact that Cu is a good conductor (5.8×10^7 S m^{-1}, 20 °C) and Cu_2O is a semiconductor, it is interesting to investigate the electric properties of such a periodically hybrid structure and to explore the possible applications of it [20–25].

In this paper we report studies on the electric properties of the nanostructured copper filaments with a conducting atomic force microscope (CAFM). By applying a constant voltage across the conducting probe of the CAFM and the sample, a current mapping is achieved, in which alternating low and high current regions correspond exactly to the periodic nanostructures on the filaments. Quantitative analysis of the current mapping also shows that there is no potential drop along the filament. A typical linear I–V curve for a metal and a nonlinear I–V curve for a semiconductor were collected in the high and low current regions respectively. These results are helpful in achieving a full understanding of the structure and the growth mechanism of the deposited filaments.

2. Experimental details

Nanostructured copper filaments, such as those shown in figure 1, were made by a unique electrodeposition method from an ultrathin layer of concentrated aqueous solution of $CuSO_4$. Details of the experimental setup and procedure were the same as reported earlier [13–15]. The morphology of the electrodeposits was characterized by a field emission scanning electron microscope (FESEM) (LEO-1530VP). For the convenience of chemical component analysis, a GaAs wafer with high electric resistance was used as a substrate. The percentage of copper and cuprous oxide in the deposited filaments was obtained by energy disperse spectroscopy (EDS) (EDAX). The electric properties of the copper filaments were measured with a high vacuum atomic force microscope (AFM) (Seiko SPI 3800N) in the conducting mode (CAFM). The principle of CAFM measurement is schematically illustrated in figure 2. The electrodeposited filaments on the substrate were connected to the metallic sample holder of the CAFM with silver paste. The metallic sample holder was held positive while the conducting cantilever of the CAFM (Si_3N_4 coated with PtIr5 from Nanoworld, AG, Switzerland) was held negative. The electric properties of the sample were measured in contacting mode. Two methods were used to characterize the electric properties of the filaments. One was current mapping, where a constant

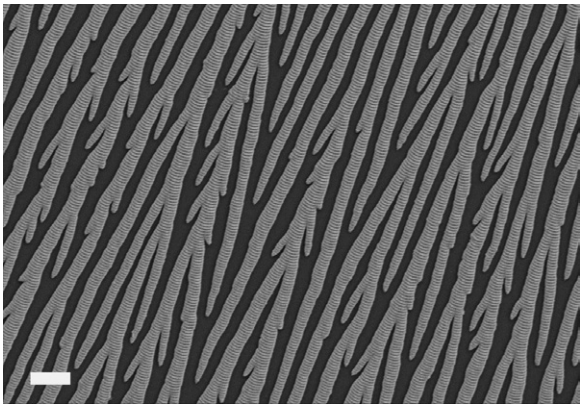

Figure 1. The SEM image of nanostructured copper filaments. (Experimental conditions: 0.05 M $CuSO_4$ electrolyte, glass substrate, 0.1 mm thick copper foil as electrode, constant voltage of 1.0 V. For experimental details see [12]). The bar represents 2 μm.

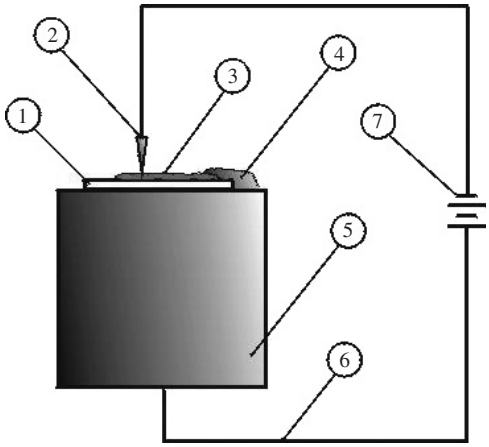

Figure 2. A schematic diagram of the kernel part of the experimental setup to measure the electric properties with a CAFM. (1) the sample holder; (2) the conducting probe of the CAFM; (3) the electrodeposited filaments; (4) the silver paste; (5) the scanner of the CAFM; ((6), (7)) inner circuit of the CAFM including the voltage supply of the CAFM.

voltage of 2.0 V was applied across the sample and the conducting probe of AFM, and the scan rate was set as 1.0 Hz. The other way was current imaging tunnelling spectroscopy (CITS). The cantilever was located at a selected spot, and the applied voltage varied from -1.0 to 1.0 V. In this way the I–V curve was obtained. The voltage scan rate was set as 50 mV s^{-1}. The electric property measurements were carried out in a high vacuum environment of 3.0×10^{-6} Torr, so the influence of water condensation on the sample surface can be avoided.

3. Results and discussion

Macroscopically the electrodeposits generated by our electrodeposition method have shiny metallic colour and grow robustly on the glass substrate. Figure 1 shows an SEM image of the deposited filaments. The branching rate of the deposits has been significantly decreased compared with those generated by conventional methods [7, 17, 18]. Even though bifurcation occurs in most of the filaments, isolated, straight filaments (more than 150 μm long) can still be observed occasionally. Figure 1 also demonstrates striking periodic corrugated structures on the filaments. It is noteworthy that the corrugation on the neighbouring filaments is synchronized in position. The coherent, periodic growth of the filaments is associated with an evident oscillation of electric current. The period of these spatiotemporal oscillations depends on the voltage applied across the electrodes, the pH of the electrolyte, and the temperature, etc [12–16].

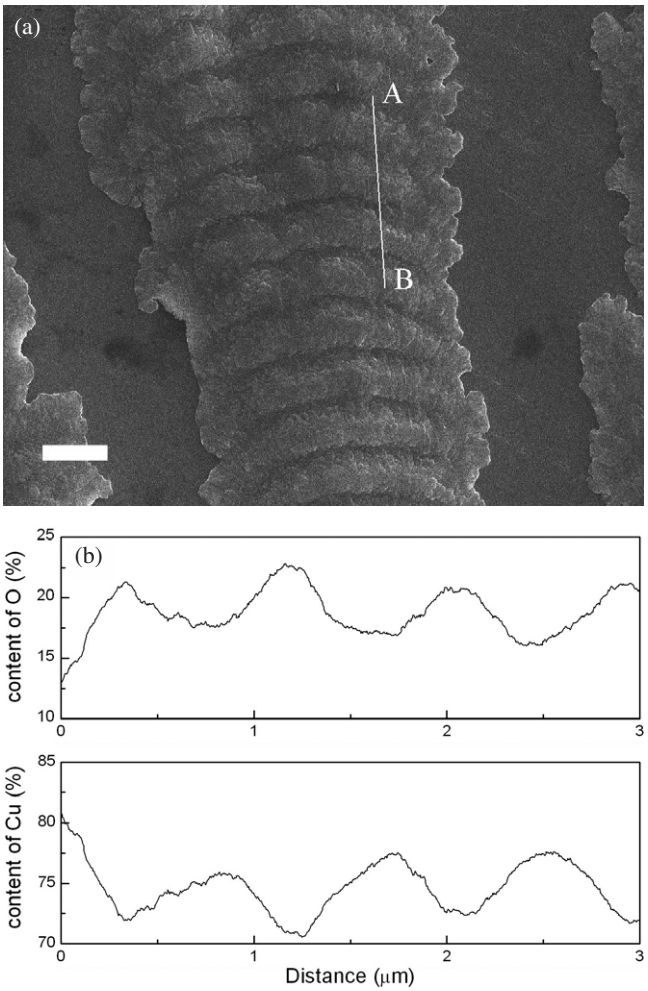

Figure 3. (a) SEM image of electrodeposited filaments grown on GaAs substrate. The bar represents 1 μm. (b) The EDS-determined content of copper and oxygen elements along the line from the point A to B marked in (a).

The chemical composition of the filaments was analysed by EDS. A single crystalline, high electric resistance GaAs wafer was used as the substrate (instead of the glass substrate) in electrodeposition for the convenience of elemental analysis. SEM topography of copper filaments on GaAs substrate, as shown in figure 3(a), reveals periodic nanostructures on the copper filament. Along the line marked in figure 3(a), the relative concentration of copper and oxygen elements were measured by EDS, as shown in figure 3(b). Corresponding to the periodic structures on the copper filaments, the ratio of copper and oxygen oscillates. The peaks and valleys of copper concentration correspond exactly to the bump and valley regions in the morphology, and the oxygen concentration is higher in the valley region and lower in the bump region. Previous transmission electron diffraction has shown that the electrodeposited filament is made of Cu and Cu_2O crystallites [12–15]. Therefore we conclude that Cu_2O crystallites are much more concentrated in the concave region than on the bump.

To investigate the electric properties of the structured filaments, a constant bias voltage was applied across the conducting AFM probe and the deposited filament such as that shown in figure 2. An AFM image of the electrodeposited filaments is shown in figure 4(a). The corresponding current image obtained with the contact mode is shown in figure 4(b). The

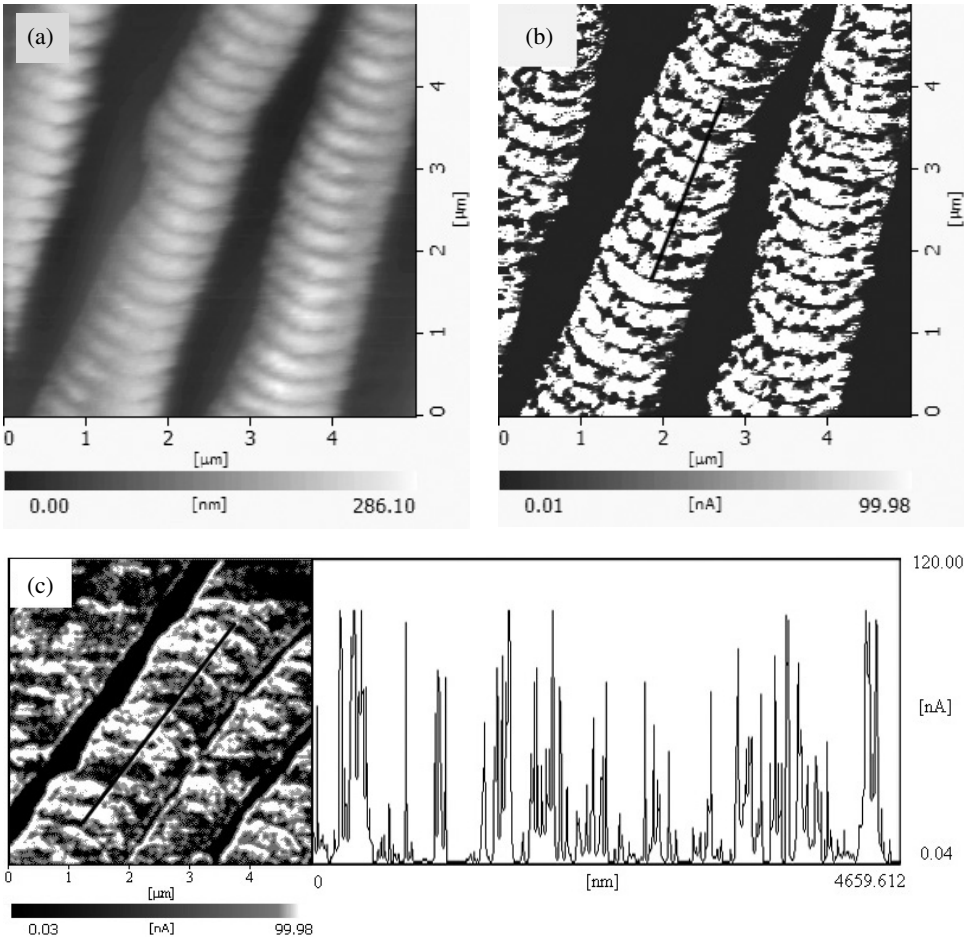

Figure 4. (a) The morphology of the copper filaments deposited on a glass substrate viewed by AFM. Periodic structures can be identified on these filaments. (b) The electric current mapping of the same filaments as those shown in (a), which was measured by a PrIr5-coated AFM probe at a scan speed of 1.0 Hz. The voltage was applied across the conducting AFM probe and the filaments was kept at 2.0 V. A periodic distribution of current density can be identified. (c) The electric current image of the filaments obtained when a lower bias of 0.8 V was applied. Quantitative analysis of the current distribution along the dark line shows that there is no potential drop along the filament.

regions with high current and low current appear alternately. The current in the concave regions is much lower than that in the bump regions. Comparing figures 4(a) and (b), one may easily find that the regions with alternating low and high electric current correspond exactly to the periodic nanostructures on the filaments. In the CAFM experiments, in order to get a clear periodic variation of electric property along the deposited filament, a higher bias (typically 1.0–2.0 V) was usually applied. However, once we tried to quantitatively analyse the current profile (and hence potential drop) along the filament, immediately we found that in the high current regions (bumps) the electric current was completely saturated. To solve this problem, a lower bias (0.8 V) was applied, and the current mapping was as shown in figure 4(c). The electric current along the black line was plotted, which indicated that there is no noticeable potential drop along the filament.

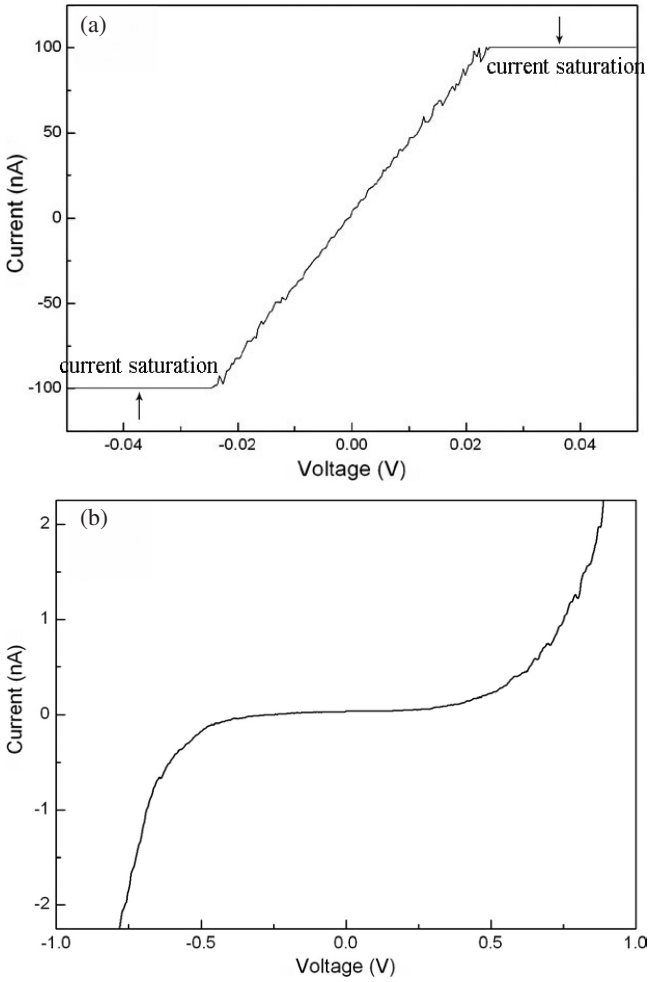

Figure 5. I–V curves measured in the bright region and in the dark region on the current mapping of the filament shown in figure 4(b). The potential scan rate was 50 mV s^{-1}. (a) In the bright region of the current mapping, a linear I–V relation can be identified. The horizontal lines are due to the saturation of electric current. (b) The nonlinear I–V relation measured in the dark region of the current mapping of the filament shown in figure 4(b).

Figure 5 is the current imaging tunnelling spectroscopy (CITS) diagram. The current–voltage relation (I–V curve) could be obtained at a selected spot. A linear I–V curve in the bump regions is shown in figure 5(a), while a nonlinear I–V curve in the concave regions of the copper filaments is shown in figure 5(b).

In previous experiments, according to the measurement of electric resistivity of the copper filaments, it was estimated that the average concentration of Cu_2O is no more than 2% [19]. Our analysis shows that the number of grains of Cu_2O crystal is high in the concave region on the deposited filaments (figure 3). On the other hand, the filaments are generated by electrochemical deposition. Therefore, all these filaments should be conductive in some way. In addition, quantitative analysis of the electric current mapping of the filaments in figure 4(c) indicated that there is no potential drop along the filament. This fact strongly suggests that there must exist conductive channels inside of the filament. Therefore the current mapping actually

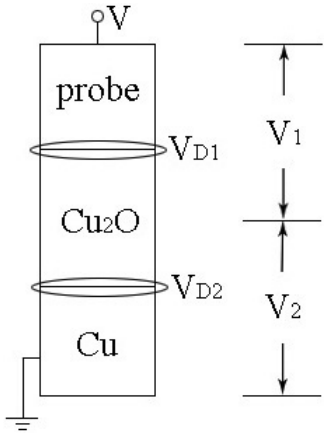

Figure 6. A schematic diagram to illustrate that the conducting probe, Cu_2O and Cu form two inversely spaced semiconductor–metal (S–M) junctions. The applied voltage V is divided to two parts, V_1 and V_2. V_1 and V_2 are applied to the junction probe–Cu_2O and the junction Cu_2O–metallic wiring, respectively. V_{D1} stands for the contact potential barrier between the probe and Cu_2O, and V_{D2} stands for the contact potential barrier between Cu and Cu_2O.

reflects the local electric property immediately under the scanning tip of the CAFM. The reason for this conclusion is that if there were no such very conductive channels inside the filaments, due to the electric resistance of the filament itself, a gradient of current density would have been observed along the filament. Therefore, our results from the conducting AFM provide important structural information on the filaments: the copper crystallites contact each other, forming conducting inner channels in the filament, whereas oscillation of the concentration field of Cu^{2+} leads to a periodic distribution of Cu_2O on the filament surface.

Based on the above experimental data, we try to establish a model for the electric property of the deposited filaments. We expect that CITS characterizes the direct electric feature of the specific point on the surface of the copper filament. Once the probe of the conducting AFM contacts a region with Cu crystal grains, a metallic conducting chain is formed, in which a part of the conducting circuits is the metallic backbone inside the filament. In this scenario a linear I–V relation such as is shown in figure 5(a) is generated. Once the scanning probe contacts a region covered with Cu_2O crystallites, a nonlinear I–V curve such as that shown in figure 5(b) is generated. A simple model to interpret the nonlinear I–V relation is illustrated in figure 6, where two semiconductor–metal (S–M) junctions are inversely connected. One junction is the junction between the conducting probe of the CAFM and Cu_2O, and the other is the junction between Cu_2O and the conducting copper channel inside the filament.

The electric properties of this system can be understood as follows. The current transport in metal–semiconductor contacts is contributed mainly by majority carriers. Cu_2O is a low-mobility semiconductor, in which diffusion theory is applicable. The diffusion theory of Schottky [26] is based on the assumption that (1) the energy barrier height of a metal–semiconductor junction is much larger than k_0T, (2) the effect of electron collisions within the depletion region is included, (3) the carrier concentrations at $x = 0$ and $x = x_d$ are unaffected by the electric current flow, and (4) the impurity concentration of the semiconductor is nondegenerate [27]. When a metal is brought into an intimate contact with a semiconductor, the determined relationship in energy levels between the semiconductor and the metal serves as a boundary condition of the Poisson equation in the semiconductor. The Poisson equations can be expressed as:

$$\begin{aligned} \frac{d^2V}{dx^2} &= \frac{qN_A}{\varepsilon_r\varepsilon_0}, \qquad -x_d \leqslant x \leqslant 0 \\ \frac{d^2V}{dx^2} &= 0, \qquad x < -x_d, \end{aligned} \tag{1}$$

where q is the electron charge, N_A is the acceptor density, ε_r is the relative dielectric constant, ε_0 is the vacuum dielectric constant, and x_d is the surface barrier layer width. $|E(x)|$ is the electric field intensity. The electric field in the semiconductor is zero, hence $|E(x_d)| = -dV/dx|_{x=-x_d} = 0$, $V(0) = \phi_{ps} = (E_F)_m/q$, where ϕ_{ps} is the height of Schottky barrier for the semiconductor, and $(E_F)_m$ stands for the Fermi energy level of the metal. In the barrier region the following relations hold:

$$\begin{aligned} |E(x)| &= -\frac{dV(x)}{dx} = -\frac{qN_A}{\varepsilon_r\varepsilon_0}(x + x_d) \\ V(x) &= \phi_{ps} + \frac{qN_A}{\varepsilon_r\varepsilon_0}\left(xx_d + \frac{1}{2}x^2\right). \end{aligned} \tag{2}$$

Since the current in the depletion region depends on the local electric field and the concentration gradient, the current density can be expressed as

$$J_x = q\left[p(x)\mu_p|E(x)| - D_p\frac{\partial p}{\partial x}\right] = -qD_p\left[\frac{qp(x)}{k_0T}\frac{\partial V(x)}{\partial x} + \frac{\partial p}{\partial x}\right] \tag{3}$$

where $p(x)$ is the carrier density, the mobility of the carrier $\mu_p = qD_p/k_0T$, and D_p is the diffusion constant. For the steady-state situation, the current density is independent of x. Equation (3) can be integrated using $\exp[qV(X)]/k_0T$ as an integrating factor. It follows that

$$J_x\int_{-x_d}^{0}\exp\left[\frac{qV(x)}{k_0T}\right]dx = -qD_p\left\{p(x)\exp\left[\frac{qV(x)}{k_0T}\right]\right\}_{-x_d}^{0}, \tag{4}$$

and the boundary conditions are

$$\begin{aligned} V(-x_d) &= \phi_{ps} - \frac{qN_A}{2\varepsilon_r\varepsilon_0}x_d^2 \\ p(-x_d) &= p_0 = N_V\exp\left(-\frac{q\phi_p}{k_0T}\right) \\ V(0) &= \phi_{ps} \\ p(0) &= p_0\exp\left[\frac{q(V_s)_0}{k_0T}\right], \end{aligned} \tag{5}$$

where N_V is the effective density of states in the valence band, p_0 is the equilibrium density of the carrier, V_s is the surface potential, and ϕ_p is the potential barrier of the metal when the metal contacts the semiconductor.

Substituting equations (5) into (4), we get

$$J_x = qD_pp_0\left\{\exp\left[\frac{q(\phi_{ps} + V_s)}{k_0T}\right]\right\}\left[\exp\left(-\frac{qV}{k_0T}\right) - 1\right]\Big/\int_{-x_d}^{0}\exp\left[\frac{qV(x)}{k_0T}\right]dx. \tag{6}$$

To get the integral in equation (6), we neglect the occurrence of x^2 in equation (2); then the potential distribution can be approximated as

$$V(x) = \phi_{ps} + \frac{qN_Ax_d}{\varepsilon_r\varepsilon_0}x. \tag{7}$$

Taking equation (7) into equation (6), the current passing through the junction can be expressed as

$$\begin{aligned} J &\cong \left\{\frac{q^2D_pN_V}{k_0T}\left[-\frac{q(V_D - V)2N_A}{\varepsilon_r\varepsilon_0}\right]^{1/2}\exp\left(-\frac{q\phi_{ps}}{k_0T}\right)\right\}\left[\exp\left(-\frac{qV}{k_0T}\right) - 1\right] \\ &= J_{SD}(V)\left[\exp\left(-\frac{qV}{k_0T}\right) - 1\right], \end{aligned} \tag{8}$$

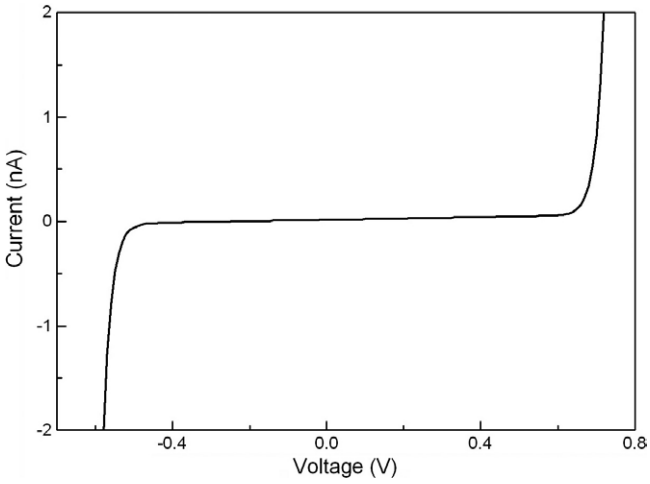

Figure 7. The calculated I–V curve based on the schematic diagram shown in figure 6 and equation (8). The following parameters are used in equation (8): V_{D1}, the contact potential barrier between Pt and Cu_2O, is 0.2 V; V_{D2}, the contact potential barrier between Cu and Cu_2O, is 0.6 V.

where V_D represents the contact potential barrier between the metal and the semiconductor, and $J_{SD}(V)$ is defined as $J_{SD}(V) = \frac{q^2 D_p N_V}{k_0 T}[-\frac{q(V_D - V)2N_A}{\varepsilon_r \varepsilon_0}]^{1/2} \exp(-\frac{q\phi_{ps}}{k_0 T})$. Clearly $J_{SD}(V)$ depends on V_D and varies with the applied voltage V. In the model of two inversely positioned S–M junctions (as shown in figure 6), the current passing through the junction between the conducting probe and Cu_2O should be equal to the current passing through Cu_2O and the conducting channel beneath. With these preparations, we are able to calculate the I–V curve. For a selected value of V, which is in between -1.0 and 1.0 V, we divide it into two parts, V_1 and V_2. V_1 and V_2 apply to the junction probe–Cu_2O and the junction Cu_2O–metallic wiring, respectively. According to equation (8) two currents are obtained. If these two currents are identical, then we shift to next V; otherwise another division of V will be made, until a correct division is reached and the currents flowing through these two junctions are identical. A simple computer code is compiled to fulfil this requirement. The value of the contact potential barrier is determined by the work function of the metal and the semiconductor, respectively, and by the detailed contact situations. For the p-type semiconductor Cu_2O, the work function of Cu_2O is larger than that of Cu and the Pt-coated probe. The work function of the Pt probe (5.3 eV) is larger than the work function of Cu (4.5 eV). For this reason, we assume V_{D1} (contact potential barrier between the probe and Cu_2O) to be smaller than V_{D2} (contact potential barrier between Cu and Cu_2O). In the calculation we set V_{D1} as 0.2 V, and V_{D2} as 0.6 V. The calculated I–V relation is shown in figure 7. It is noteworthy that this curve is not symmetrical about the point $V = 0$. A similar tendency has been experimentally observed, such as that shown in figure 5(b). As a matter of fact, as long as the contact potential barriers V_{D1} and V_{D2} are different, an asymmetric I–V curve should be expected.

In our previous studies of electrodeposited filaments, we knew that the spatial distribution of Cu_2O and Cu varied periodically and followed the corrugated structures on the filament surface. However, we did not know the exact location of the crystallites of copper/cuprous oxide in the filament. More specifically, for the regions where we detected a high concentration of Cu_2O, we did not know whether the crystallites of Cu_2O distributed homogeneously across the filament, or Cu_2O existed only on the surface of the filament. The mapping of the electric properties of the filaments shown in this paper helps to clarify the structure of the electrodeposits. We can conclude now that Cu_2O is periodically concentrated on the surface layer of the filament. This unique structure implies possible applications. Suppose that an electric current with sufficiently high frequency is applied to such a structured filament.

The current density tends to be higher on the surface of copper filaments (known as skin effect) [28–31]. With such a skin effect, the copper filaments eventually become an array of metal–semiconductor junctions, and they might be used as unidirectional current-carrying devices, such as rectifier elements.

4. Summary

We report in this article the electric characterization of nanostructured copper filament arrays, which are self-organized by a novel electrochemical method. An alternating distribution of crystallites of copper and cuprous oxide appears on the deposited filaments. The electric current mapping of the filaments helps to pinpoint the structure of the deposited filaments. We conclude that Cu_2O is periodically concentrated on the surface layer of the filament. Such a unique structure might have potential applications in high frequency rectifier devices.

Acknowledgments

This project was supported by the NSF of China (10021001 and 10374043) and the Ministry of Science and Technology (2004CB619005). MW would also like to thank the support of Ecole Polytechnique, where conducting AFM experiments on deposited filaments were initiated.

References

[1] Edelstein D *et al* 1997 *Tech. Dig. Int. Electron Devices Meet.* **1997** 773
[2] Venkatesan S *et al* 1997 *Tech. Dig. Int. Electron Devices Meet.* **1997** 769
[3] Gurtner C and Sailor M 1996 *Adv. Mater.* **8** 897
[4] Bradley J *et al* 1997 *Nature* **389** 268
[5] Curtis C *et al* 1993 *Science* **262** 2014
[6] Sailor M and Curtis C 1994 *Adv. Mater.* **6** 688
[7] Fleury V *et al* 1994 *Nature* **367** 435
[8] Wang M *et al* 1994 *Nature* **367** 438
[9] Huth J M *et al* 1995 *Phys. Rev.* E **51** 3444
[10] de Bruyn J R 1995 *Phys. Rev. Lett.* **74** 4843
[11] Zhang K-Q *et al* 2000 *Phys. Rev.* E **61** 5512
[12] Wang M *et al* 2001 *Phys. Rev. Lett.* **86** 3827
[13] Zhong S *et al* 2003 *Phys. Rev.* E **67** 061601
[14] Wang M *et al* 2004 *Surf. Interface Anal.* **36** 197
[15] Wang Y *et al* 2004 *Phys. Rev.* E **69** 021607
[16] Snow E and Campbell P 1994 *Appl. Phys. Lett.* **64** 1932
[17] Fleury V *et al* 2002 *Nature* **416** 716
[18] Hibbert D B and Melrose R 1988 *Phys. Rev.* A **38** 1036
[19] Zhong S *et al* 2001 *J. Phys. Soc. Japan* **70** 1452
[20] Chatterjee K *et al* 2004 *J. Appl. Phys.* **96** 683
[21] Ban D and Sargent E 2002 *Appl. Phys. Lett.* **81** 5057
[22] Suku K *et al* 2004 *Electrochem. Solid State Lett.* **7** G145
[23] Trenkler T *et al* 2000 *J. Vac. Sci. Technol.* B **18** 586
[24] Hunger T *et al* 2004 *Phys. Rev.* B **69** 195406
[25] Tang X *et al* 2004 *Appl. Phys. Lett.* **84** 3043
[26] Schottky W 1938 *Naturwissenschaften* **26** 843
[27] Sze S M 1981 *Physics of Semiconductor Device* 2nd edn (New York: Wiley) chapter 5
[28] Wall D and Allen J 2005 *J. Appl. Phys.* **98** 023304
[29] Saguy H and Rittel D 2005 *Appl. Phys. Lett.* **87** 084103
[30] Phan M *et al* 2005 *J. Appl. Phys.* **98** 014316
[31] Hagelaar G *et al* 2004 *J. Appl. Phys.* **96** 1819